scientific reports

Check for updates

OPEN

Fluorofenidone attenuates choline-deficient, l-amino acid-defined, high-fat diet-induced metabolic dysfunction-associated steatohepatitis in mice

Jian Zhang[1], Qianbing Wang[1], Nianqi Zhou[1], Jinqing Liu[1], Lijian Tao[3], Zhangzhe Peng[3], Gaoyun Hu[4], Huiwen Wang[2]✉, Lei Fu[1]✉ & Shifang Peng[1]✉

Metabolic dysfunction-associated steatohepatitis (MASH), a severe form of metabolic dysfunction-associated steatotic liver disease (MASLD), involves hepatic lipid accumulation, inflammation, and fibrosis. It can progress to cirrhosis or hepatocellular carcinoma without timely treatment. Current treatment options for MASH are limited. This study explores the therapeutic effects of fluorofenidone (AKF-PD), a novel small-molecule compound with antifibrotic and anti-inflammatory properties, on MASH in mouse model. Mice fed a choline-deficient, l-amino acid-defined, high-fat diet (CDAHFD) were treated with AKF-PD, resulting in reduced serum ALT, AST, hepatic lipid accumulation, liver inflammation, and fibrosis. Network pharmacology and RNA-sequencing analyses suggested that AKF-PD influenced multiple metabolic, inflammatory, and fibrosis-related pathways. Further experiments verified that AKF-PD activated hepatic AMPK signaling, leading to the inhibition of the downstream SREBF1/SCD1 pathway and the activation of autophagy. Additionally, AKF-PD suppressed the expression of various inflammatory factors, reduced macrophage infiltration, and inhibited NLRP3 inflammasome activation. Moreover, AKF-PD attenuated liver fibrosis by inhibiting TGFβ1/SMAD signaling. In conclusion, this study reveals that AKF-PD effectively decreases hepatic lipid accumulation, liver inflammation and fibrosis in a CDAHFD-induced MASH model, positioning AKF-PD as a promising candidate for the treatment of MASH.

Keywords Metabolic dysfunction-associated steatotic liver disease, Metabolic dysfunction-associated steatohepatitis, Fluorofenidone, AMPK, NLRP3 inflammasome, TGFβ1/SMAD pathway

Metabolic dysfunction-associated steatotic liver disease (MASLD) encompasses a spectrum of liver disorders characterized by hepatic steatosis in more than 5% of hepatocytes[1,2]. Metabolic dysfunction-associated steatohepatitis (MASH) represents a more severe form of MASLD, featuring hepatocellular injury (ballooning), lobular inflammation, and varying degrees of fibrosis[1,3]. MASLD affects about 25% of people globally[4], of whom 20% have MASH and are at risk of developing cirrhosis and/or hepatocellular carcinoma (HCC) without timely intervention[5,6]. While MASH can be improved through diet control and proper exercise, the long-term sustainability of these interventions is a significant challenge[7]. Additionally, liver fibrosis, a major complication of MASH, is difficult to reverse[8]. To date, treatment options for MASLD are limited, underscoring the urgent need for an effective drug, particularly for MASH.

The pathogenesis of MASH is complex and multifactorial. Several studies consider overnutrition, which causes excess hepatic lipid accumulation, as the primary driver of MASLD[9–11]. This lipid imbalance results in the formation of lipotoxic species, which induce cellular stress, inflammasome activation, and apoptosis, ultimately promoting liver inflammation and fibrosis[1,12]. Macrophages are especially vital to the progression

[1]Department of Infectious Diseases, Xiangya Hospital, Central South University, Changsha 410008, Hunan, China. [2]Department of Infection Control Center, Xiangya Hospital, Central South University, Changsha 410008, Hunan, China. [3]Department of Nephrology, Xiangya Hospital, Central South University, Changsha 410008, Hunan, China. [4]Faculty of Pharmaceutical Sciences, Central South University, Changsha 410008, Hunan, China. ✉email: huiwenwang0325@163.com; fulei92@126.com; sfp1988@csu.edu.cn

of liver fibrosis and inflammatory processes[13]. Current pharmaceutical research was focused on blocking lipid metabolism, inflammation, and fibrosis, key processes involved in MASLD pathogenesis. However, the treatment of MASLD/MASH remains a clinical challenge. In patients with obesity or type 2 diabetes, incretin mimetics such as specifically glucagon-like peptide-1 (GLP-1) receptor agonists (GLP-1RAs) and insulin sensitizers like pioglitazone may provide some benefit. Emerging evidence suggests that these agents can alleviate steatohepatitis and reduce cardiovascular risks, but their efficacy in improving liver fibrosis remains unsatisfactory[14–16]. Resmetirom, the only FDA-approved pharmacotherapy for MASH without cirrhosis, has shown promise but requires further investigation to evaluate its long-term safety, particularly concerning endocrine-related adverse effects on the thyroid glands, gonads, and bones[16]. Accordingly, it remains critical to explore more safe and effective drugs.

Fluorofenidone [1-(3-fluorophenyl)-5-methyl-2-(1H)-pyridone; AKF-PD] is a novel small-molecule compound originally developed to treat renal fibrosis by blocking TGFβ signaling[17–19]. Subsequent studies have demonstrated its effectiveness in treating liver fibrosis by suppressing the NF-κB pathway and hepatic stellate cell activation[20,21] as well as pulmonary fibrosis by inhibiting NLRP3 inflammasome activation and eIF3a expression[22,23]. Additionally, AKF-PD exhibits potent anti-inflammatory properties by inhibiting inflammasome activation, the MAPK/NF-κB pathway, and the release of pro-inflammatory cytokines such as TNF-α and IL-1β[22,24–26]. Our previous study reported that AKF-PD ameliorates cholestasis, a chronic liver disease characterized by the intrahepatic accumulation of bile acids[27]. More importantly, alleviating cholestasis in MASH patients is also considered an effective therapeutic strategy[28,29]. Compared to current treatments, which are limited by their single-target focus and inability to reverse severe MASH, AKF-PD's powerful effects of anti-inflammation, anti-fibrosis, and anti-cholestasis highlight its significant therapeutic potential for patients with advanced liver injury and fibrosis. However, it remains unclear whether AKF-PD can effectively protect against MASH.

This study investigated the therapeutic potential of AKF-PD in a mouse model of MASH induced by a choline-deficient, L-amino acid-defined, high-fat diet (CDAHFD). Using an integrated approach combining bioinformatics analysis and *in vivo* experiments, we aimed to verify whether AKF-PD could attenuate hepatic injury, steatosis, inflammation, and fibrosis. By elucidating its effects and underlying mechanisms, this study may provide new insight into the development of AKF-PD as a potential treatment for MASH.

Results

AKF-PD alleviates liver injury and hepatic lipid accumulation in mice

To determine the effect of AKF-PD on MASH, mice were divided into three groups: chow diet, CDAHFD + vehicle, or CDAHFD + AKF-PD (Fig. 1A). The dose and administration method of AKF-PD were established based on prior studies and our group's previous findings (In vivo, we evaluated the doses of AKF-PD by 125, 500 and 1000 mg/kg, and found that 500 mg/kg of AKF-PD was provided the desired therapeutic effects)[27,30]. Liver weight (LW) and liver weight/body weight (LW/BW) measurements suggested that AKF-PD treatment reduced the enlarged liver induced by CDAHFD (Fig. 1B). Consistent with previous reports, CDAHFD-fed mice had a lower fasting blood glucose and body weight than those fed the chow diet alone[31,32], but neither could be restored by AKF-PD treatment (Fig. 1C). More importantly, AKF-PD significantly reduced serum ALT and AST levels compared to vehicle-treated CDAHFD mice (Fig. 1D, Table 1). Recent studies have highlighted the vital role of cholestasis in MASLD[28,29,33,34]. We also found that AKF-PD lowered serum TBA levels in CDAHFD-fed mice (Fig. 1D), consistent with our previous findings in cholestasis[27]. Histological analysis of H&E and Oil-red staining showed excessive inflammation and lipid droplets in the CDAHFD group, which were obviously alleviated by AKF-PD treatment (Fig. 1E). Liver TG and TC levels were also markedly downregulated in the AKF-PD treatment group (Fig.1F, Table 1). Moreover, the nonalcoholic fatty liver disease (NAS) score, a histological score widely used in the clinic, was significantly improved by AKF-PD treatment (Fig. 1G). Collectively, these findings indicated that AKF-PD could alleviate liver injury and hepatic lipid accumulation in MASH.

Network pharmacology and RNA-sequencing analyses reveal that AKF-PD may improve MASH by targeting AMPK and NLRP3 inflammasome signaling

To further identify the underlying mechanism, we performed network pharmacology analysis to predict potential targets. We searched for the pathogenic genes of MASLD and the targets of AKF-PD from different databases and used common genes for enrichment analysis. A total of 2,738 pathogenic genes of MASLD and 47 target genes of AKF-PD were identified, of which 15, were common to both (Fig. 2A). Enrichment analysis of 15 genes using the KEGG and Reactome databases suggested these genes involved metabolic and inflammatory-related pathways (Fig. 2B). RNA-sequencing of mouse liver samples further supported these findings. The principal component analysis (PCA) plot indicated a clear distinction between the vehicle and AKF-PD groups (Fig. 2C). Volcano plot analysis revealed 1614 differentially expressed genes (DEGs) between the two groups (Fold Change ≥ 1.5, $p < 0.05$). Among these, 672 DEGs were upregulated, including genes involved in lipid utilization, such as *Acad1, Acot1, Cyp4a10,* and *Cyp4a14*. Moreover, a total of 942 DEGs were downregulated, including pro-inflammatory genes (*Cxcl5, Ccr7,* and *Cxcl14)*, lipogenesis genes (*Fasn* and *Srebf1*), and fibrosis-related genes (*Col1a1, Col1a2, Tgfb1, Tgfb2, Acta2,* and *Ctgf*) (Fig. 2D). Consistent with the results of network pharmacology analysis, KEGG and Reactome enrichment analyses of these DEGs indicated that they were closely associated with metabolic, inflammatory, and fibrosis-related biological processes (Fig. 2E). Interestingly, both analyses involved the enrichment of AMPK and NLRP3 inflammasome pathways. Based on these findings, we hypothesized that AKF-PD alleviates MASH by modulating these pathways and investigated further.

AKF-PD reduces hepatic lipid accumulation by targeting AMPK signaling

To confirm how AKF-PD modulates lipid homeostasis, we assessed the expression of key lipid metabolism genes. Heatmap analysis revealed that AKF-PD decreased lipogenesis-related genes while promoting lipolysis

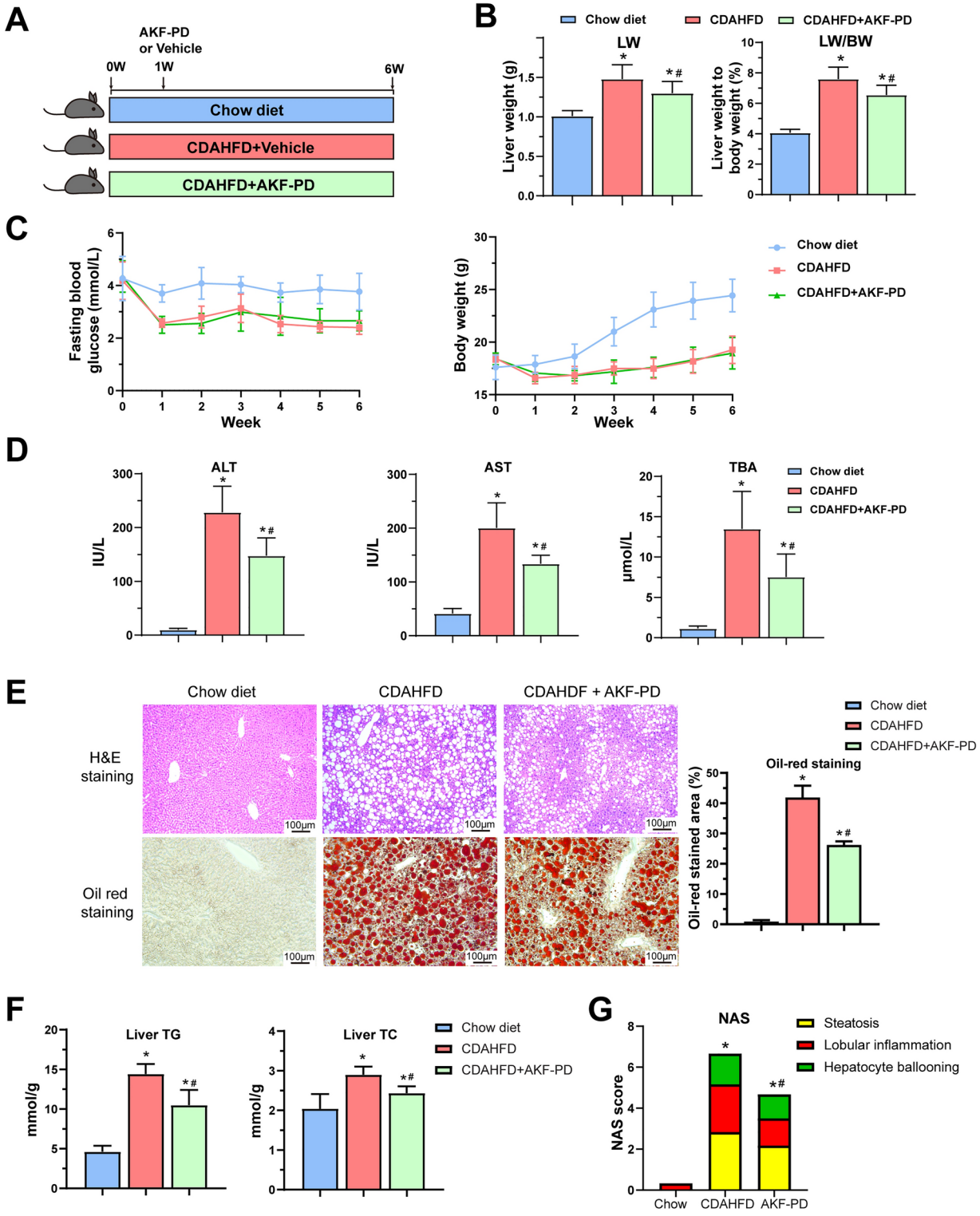

Fig. 1. AKF-PD alleviates liver injury and hepatic lipid accumulation in mice. (**A**) Schematic of the experimental procedure used to explore the effect of AKF-PD on a CDAHFD-induced MASH mouse model (n=6/group); (**B**) LW and LW/BW ratio of mice; (**C**) Fasting blood glucose and body weight of mice; (**D**) Serum ALT, AST, and TBA levels in different groups. (**E**) Representative H&E, Oil-red staining images, along with quantification of Oil-red staining in liver samples (Magnification, ×100. Bar = 100 μm.); (**F**) Liver TG and TC levels of each group (n=6/group); (**G**) NAS score of each group. Data are expressed as the mean ± SD. A one-way ANOVA analysis was used for statistical analysis. * p <0.05 as compared with the chow diet group; #p <0.05 as compared with the CDAHFD group.

	Chow diet (n=6)	CDAHFD (n-6)	CDAHFD+AKF-PD (n=6)
Serum ALT (IU/L)	9.95±2.68	228.20±2.68*	147.60±33.27*#
Serum AST (IU/L)	40.98±9.59	200.30±46.67*	133.60±16.00*#
Serum TBA (μmol/L)	1.13±0.31	13.48±4.65*	7.53±2.84*#
Liver TG (mmol/g)	4.63±0.74	14.42±1.26*	10.49±1.91*#
Liver TC (mmol/g)	2.04±0.37	2.90±0.20*	2.43±0.18#

Table 1. Serum and Liver Biochemistry. Values are the means ± SD.*P <0.05 versus Chow diet mice and #P <0.05 versus CDAHFD; Groups were compared using a one-way ANOVA. *AKF-PD* Fluorofenidone, *ALT* alanine aminotransferase, *AST* aspartate aminotransferase, *TBA* total bile salts, *TG* triglyceride, *TC* total cholesterol.

(Fig. 3A). RT-qPCR analysis validated the significant downregulation of lipogenesis-related genes, including *Scd1, Plin2, Plin3, Plin4, Cidea, and Cidec* (Fig. 3B). SREBF1/SCD1 signaling is involved in lipogenesis regulated by AMPK[35,36]. RNA-sequencing data confirmed that AKF-PD could decrease the expression of *Srebf1* and *Scd1* (Fig. 3A). Further western blot analysis verified that the protein levels of SREBF1 and SCD1 could be dramatically reduced by AKF-PD treatment (Fig. 3C). The p-AMPK/AMPK ratio was significantly increased, while the downstream p-mTOR/mTOR was decreased in the AKF-PD treatment group, suggesting that AKF-PD could activate AMPK signaling in the CDAHFD-induced MASH model (Fig. 3C). Autophagy, one of the predicted targets identified by the network pharmacology analysis, is an intracellular degradation system that removes lipid droplets from hepatocytes[37–39]. This process is activated by AMPK and inhibited by mTOR signaling[40,41]. The western blot analysis revealed that AKF-PD increased the expression of autophagy markers, as evidenced by decreased p62 levels and an increased LC3-II/LC3-I ratio (Fig. 3D). These findings together suggest that AKF-PD reduces liver lipid accumulation by activating AMPK signaling in MASH.

AKF-PD ameliorates liver inflammation by inhibiting macrophage infiltration and the NLRP3 inflammasome

Previous studies have reported that AKF-PD has powerful anti-inflammatory effects in different diseases. Our RNA-sequencing results also confirmed this, revealing the downregulation of numerous inflammation-related genes (Fig. 4A). RT-qPCR further confirmed that AKF-PD significantly reduced the expression of inflammatory mediators such as *Tnfα, Il1β, Il6, Ccl2, Cxcr2,* and *Cxcl10* (Fig. 4B). Given the vital role of macrophages in MASH and liver fibrosis, we assessed macrophage infiltration via immunofluorescence staining. AKF-PD treatment markedly attenuated macrophage infiltration in CDAHFD-fed mice (Fig. 4C). Since the NLRP3 inflammasome is crucial for macrophage activation in MASH and it was one of the most significant predicted targets identified by both network pharmacology and RNA-sequencing analysis, we examined its activation in liver tissues. Further experiments showed that effectively AKF-PD restored the elevated protein levels of NLRP3, Caspase1, ASC, and IL-1β induced by CDAHFD (Fig. 4D, Fig. S1). In summary, these findings suggested that AKF-PD ameliorates inflammation by inhibiting macrophage infiltration and the NLRP3 inflammasome activation in MASH.

AKF-PD attenuates liver fibrosis by suppressing TGFβ1/SMAD signaling

The powerful anti-fibrosis function of AKF-PD has been identified in many diseases[17,19,21,27], but its impact on MASH-associated fibrosis remains unclear. Sirius red staining revealed that AKF-PD successfully improved liver fibrosis induced by CDAHFD (Fig. 5A). RNA-sequencing data indicated that AKF-PD attenuated the expression of many fibrotic genes (Fig. 5B). Validation by RT-qPCR confirmed that AKF-PD reduced the expression of classic liver fibrotic genes, including *α-Sma, Pdgfβ, Tgfβ1, Col1a1, Col1a2, Mmp2, Mmp9, Ctgf,* and *Timp1* (Fig. 5C). Western blot analysis further demonstrated that AKF-PD suppressed PDGFR-β and α-SMA protein levels, two fibrogenesis markers (Fig. 5D). TGFβ1/SMAD signaling is the dominant pathway involved in fibrogenesis[42]. Our previous study found that AKF-PD blocked TGFβ1/SMAD signaling in cholestasis-induced liver fibrosis[27]. It showed that AKF-PD also inhibited the phosphorylation of SMAD2 and SMAD3, key effectors of TGFβ1 signaling in MASH (Fig. 5D). These data suggest that AKF-PD attenuates liver fibrosis by targeting the TGFβ1/SMAD signaling in MASH.

Discussion

MASLD, and especially MASH, causes serious disease burden worldwide, but the effective treatments are limited. This study provides the first *in vivo* evidence that AKF-PD significantly improves CDAHFD-induced MASH model by reducing hepatic lipid, liver inflammation, and fibrosis. Mechanically, AKF-PD decreased hepatic lipid accumulation by activating AMPK, alleviated liver inflammation by suppressing macrophage infiltration and the NLRP3 inflammasome activation, and ameliorated liver fibrosis by inhibiting TGFβ1/SMAD signaling (Fig. 6). AKF-PD may thus serve as a potential candidate drug for the treatment of MASH.

CDAHFD is a widely accepted and adopted mouse model in the studies of MASLD/MASH. It can induce obvious hepatic steatosis, liver injury, inflammation, and fibrosis after 6 weeks of feeding[31]. In contrast, other commonly used models, such as the high-fat diet or high-fat, fructose, and cholesterol models, while inducing obesity and insulin resistance, require prolonged feeding (over 20 weeks) to develop liver injury and are less prone to fibrogenesis. Additionally, our ongoing study has found that AKF-PD activates the PPAR signaling (data not shown), which is associated with obesity and insulin resistance in MASH, reflecting its potential effect

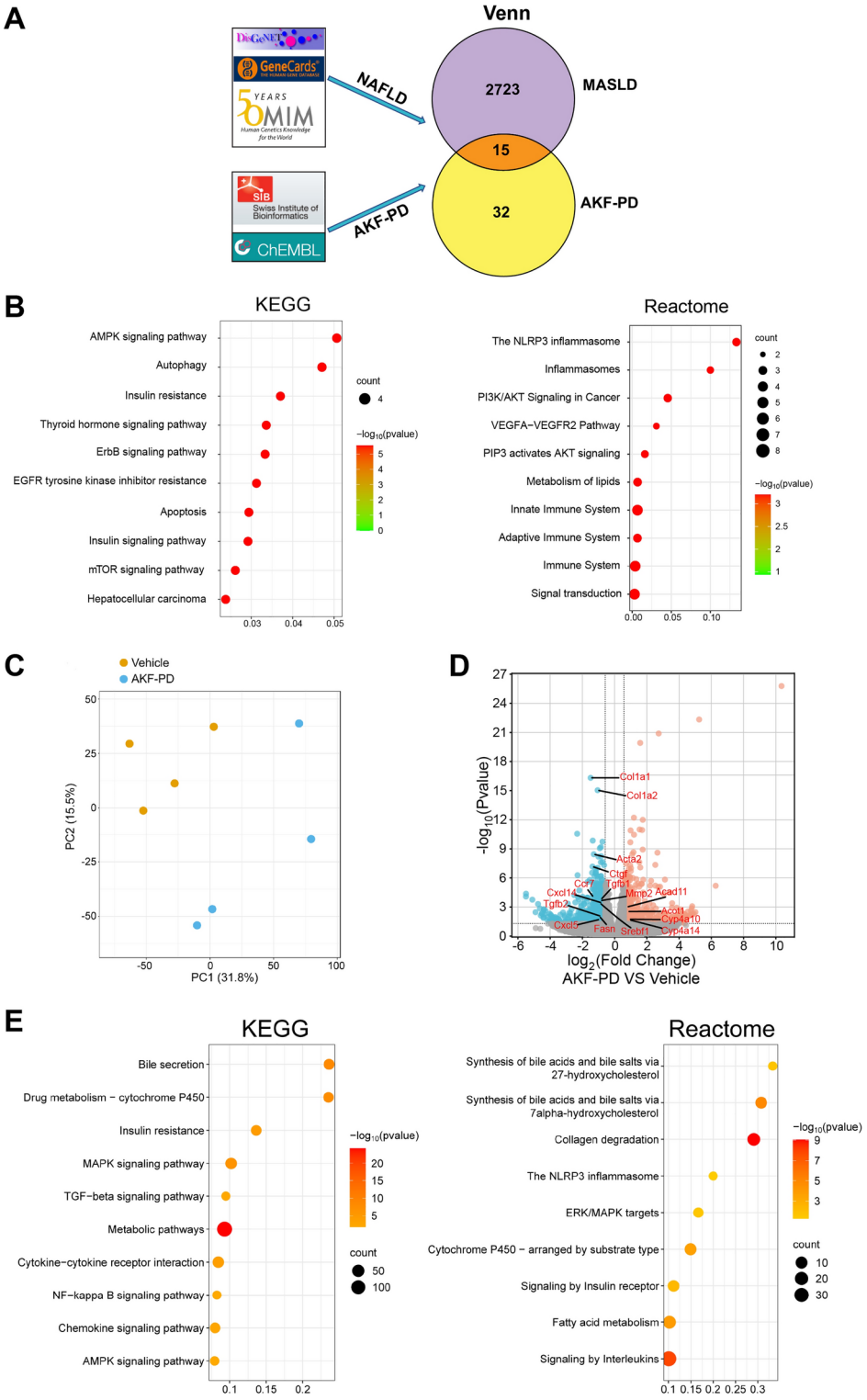

Fig. 2. Integration of network pharmacology and RNA-sequencing analysis reveals that AKF-PD may alleviate MASH by targeting AMPK and the NLRP3 inflammasome. (**A**) Diagram illustrating the use of flowcharts to prioritize AKF-PD biotargets and signaling pathways against MASH using a network pharmacology approach; (**B**) Enrichment analysis of 15 targets using the KEGG and Reactome databases. (**C**) PCA map shows the distribution of expression values between the Vehicle and AKF-PD group based on liver RNA-sequencing data (n=4/group). (**D**) Volcano map of all DEGs. $P < 0.05$ and | Fold Change |≥ 1.5 were considered threshold values for significant DEGs. (**E**) Enrichment analysis of all DEGs using the KEGG and Reactome databases.

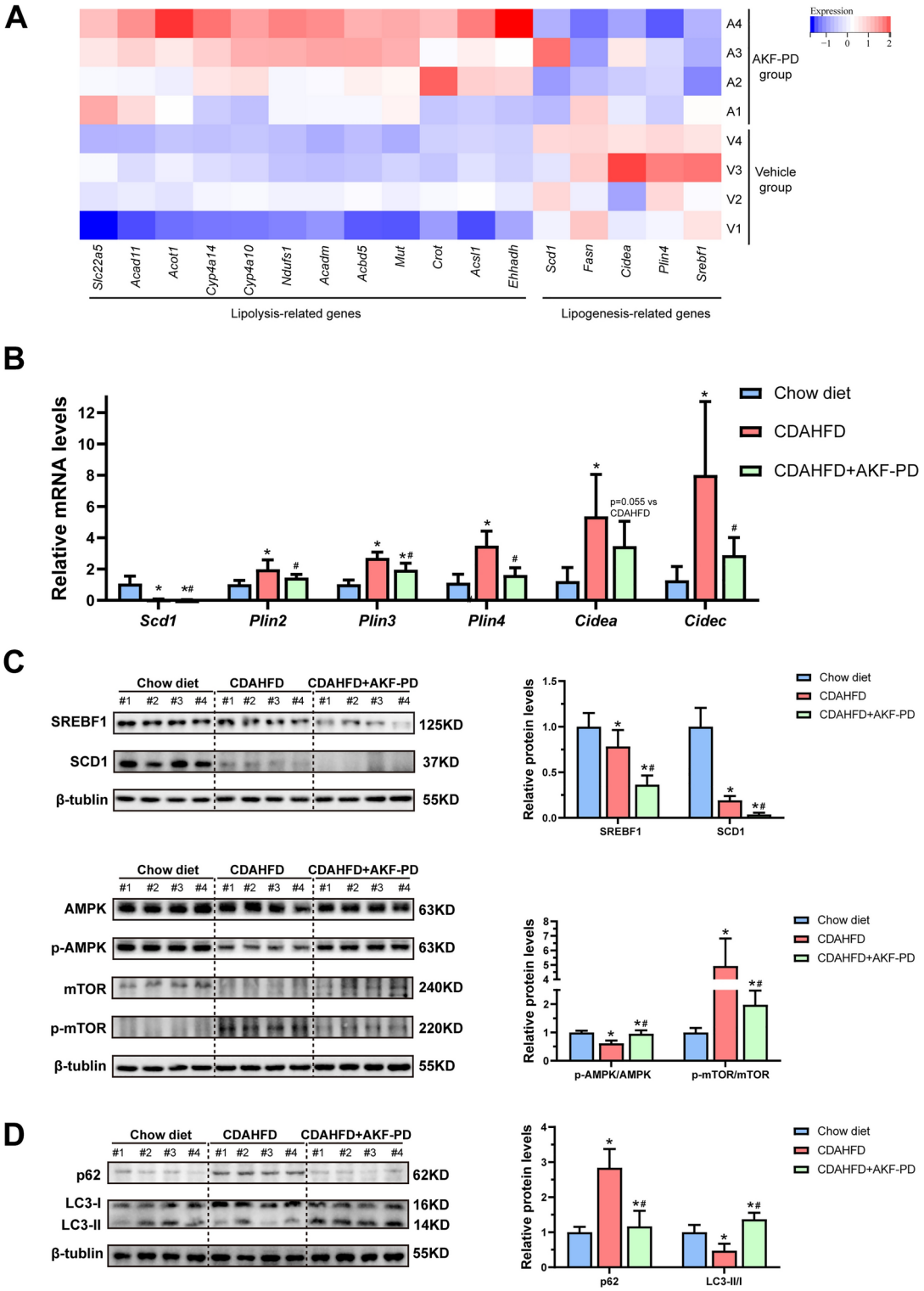

Fig. 3. AKF-PD reduces hepatic lipids in mice by activating AMPK. (**A**) Heatmap of lipolysis and lipogenesis-related genes from hepatic RNA-sequencing results. (**B**) RT-qPCR analysis of the hepatic mRNA levels of key genes involved in lipid metabolism (n=6/group). (**C**, **D**) Representative western blot analysis and quantitative data associated with SREBF1/SCD1 signaling, AMPK/mTOR signaling, and autophagy (n=6/group). A one-way ANOVA analysis was used for statistical analysis. *p <0.05 as compared with the chow diet group; #p <0.05 as compared with the CDAHFD group.

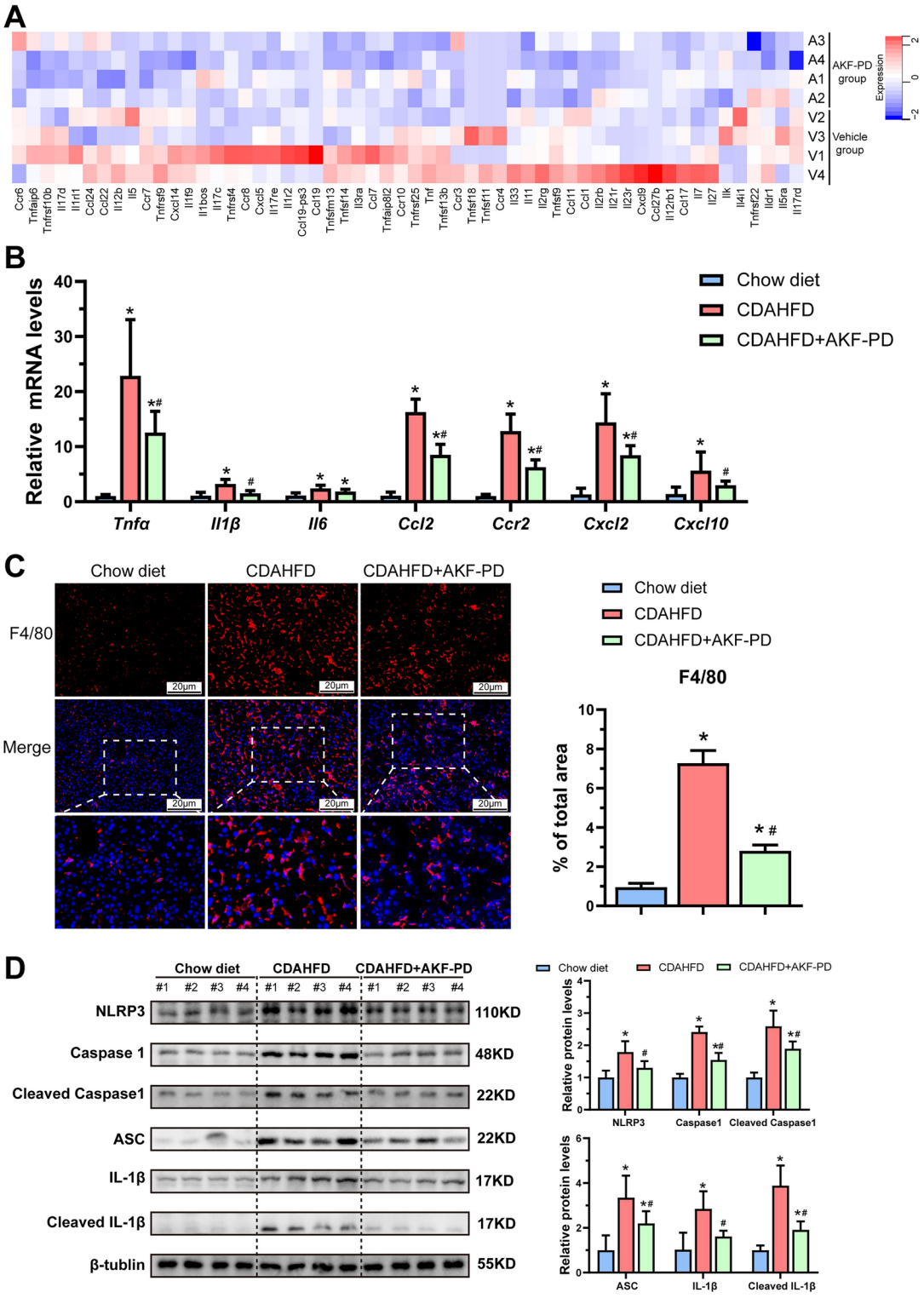

Fig. 4. AKF-PD improves liver inflammation by inhibiting macrophage infiltration and the NLRP3 inflammasome activation. (**A**) Heatmap of inflammation-related genes from hepatic RNA-sequencing results. (**B**) RT-qPCR analysis of the hepatic mRNA levels of several pro-inflammatory factors (n=6/group); (**C**) Representative IF staining and quantification using F4/80 (red) and nuclei labeled with DAPI (blue) (n=3/group. Magnification, ×200. Bar = 20 μm.); (**D**) Representative western blot images and corresponding densitometry of the NLRP3 inflammasome (NLRP3, Caspase1, Cleaved Caspase1, ASC, IL-1β, and Cleaved IL-1β) from mouse liver tissue lysates obtained from each group (n=6/group). A one-way ANOVA analysis was used for statistical analysis. *p <0.05 as compared with the chow diet group; #p <0.05 as compared with the CDAHFD group.

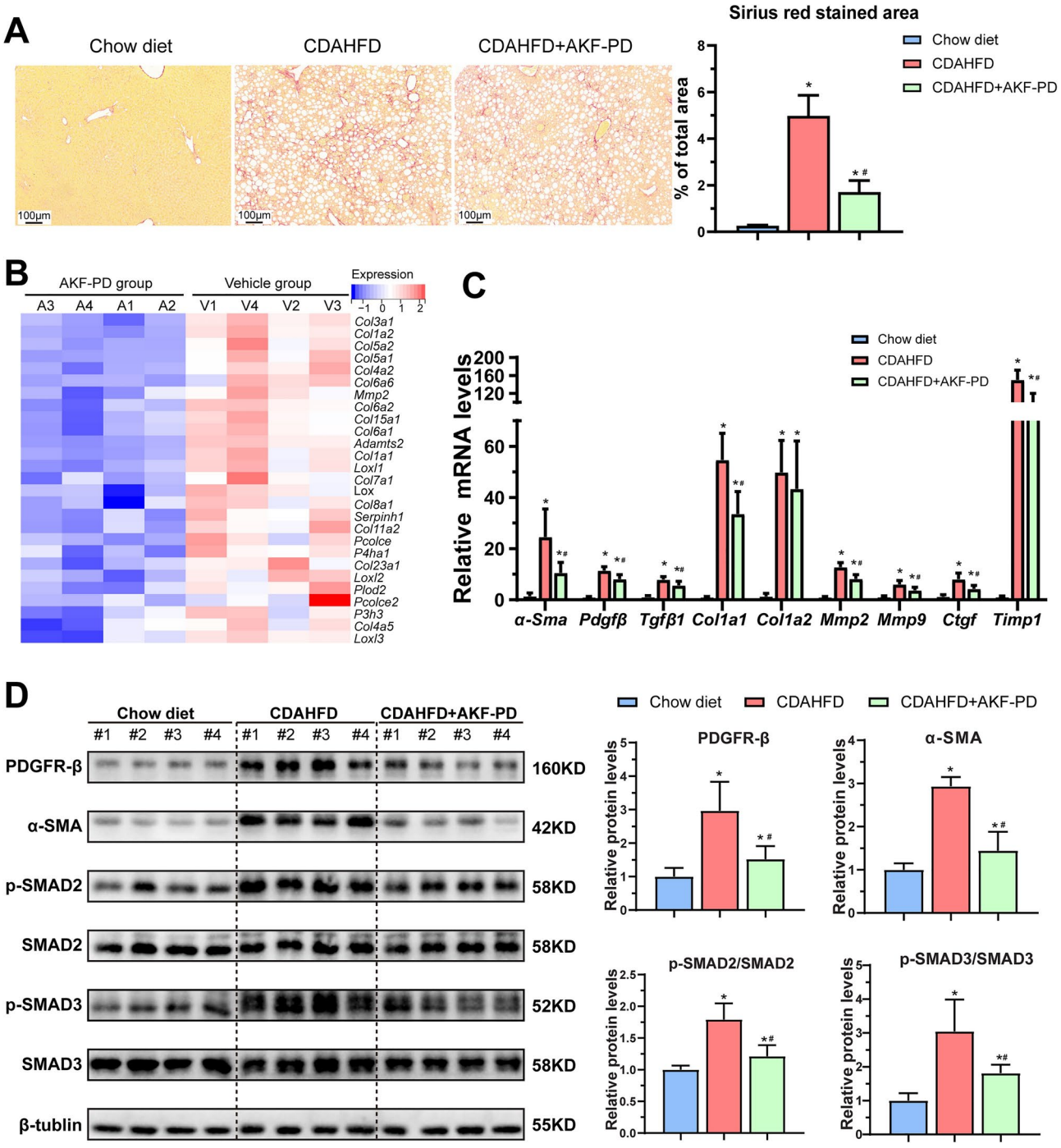

Fig. 5. AKF-PD ameliorates liver fibrosis by suppressing TGFβ1/SMAD signaling. (**A**) Representative Sirius red staining and quantification of liver tissues in different groups (n=3/group. Magnification, ×100. Bar = 100 μm.); (**B**) Heatmap of fibrosis-related genes from hepatic RNA-sequencing results. (**C**) RT-qPCR analysis of the hepatic mRNA levels of profibrogenic genes (n=6/group); (**D**) Representative western blots and corresponding quantification of PDGFR-β, α-SMA, p-SMAD2, SMAD2, p-SMAD3, and SMAD3 from mouse liver tissue lysates (n=6/group). A one-way ANOVA analysis was used for statistical analysis. *p <0.05 as compared with the chow diet group; #p <0.05 as compared with the CDAHFD group.

on modulating insulin resistance. Although the CDAHFD model does not show some extrahepatic MASLD characteristics such as hyperglycemia and hyperlipidemia, the intrahepatic lesions in this model were severe. The severity of liver injury and fibrosis makes CDAHFD model more consistent with the pathological features of MASH in humans. Moreover, therefore, it is a suitable choice for studying the effects and mechanisms of drugs on the severe liver lesions of MASH.

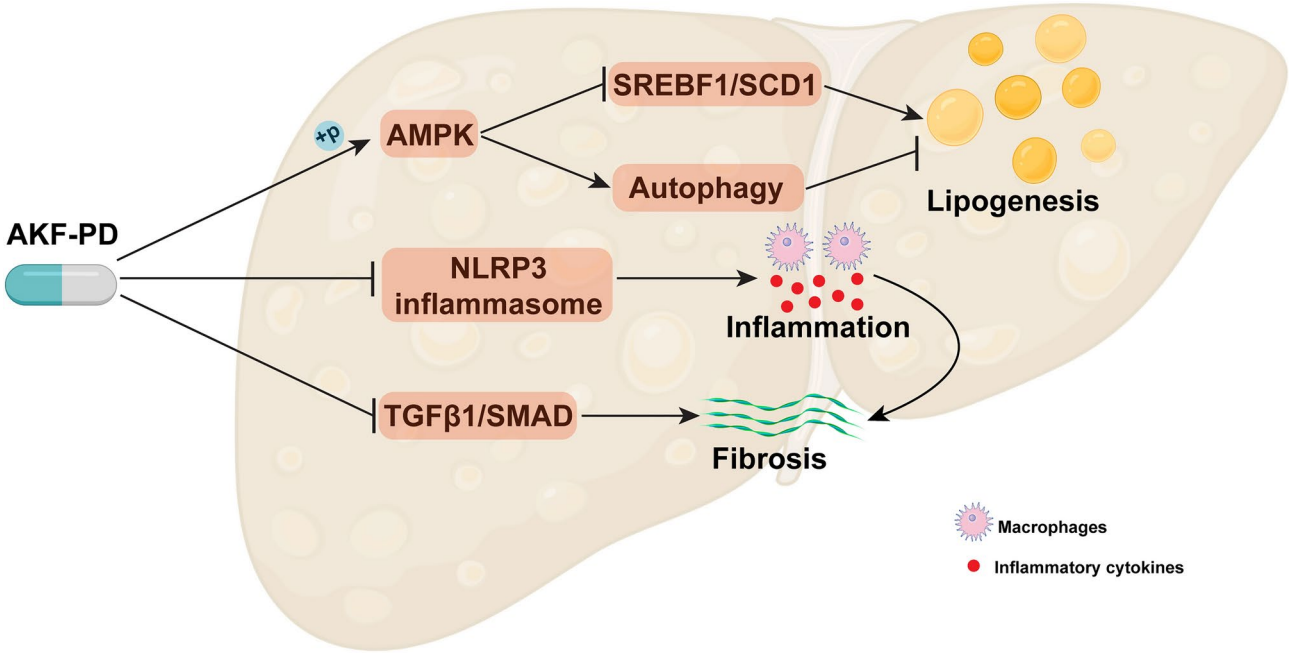

Fig. 6. Diagram of the AKF-PD mechanism. AKF-PD attenuates hepatic lipids accumulation, inflammation, and fibrosis in a mouse model of MASH by targeting AMPK, inflammasome activation, and TGFβ1/SMAD signaling.

The accumulation of excess lipids in the liver is a hallmark of MASLD. These toxic lipids induce hepatocellular injury and fibrosis and can lead to the development of cirrhosis or HCC[1]. AMPK is a major energy sensor that suppresses particular enzymes or transcription factors critical for controlling lipid biosynthesis[43] and is a promising target for MASLD[43–46]. Our data showed that AKF-PD could restore the activity of AMPK pathway in the MASH mouse model. Specifically, AKF-PD was shown to suppress AMPK/SREBF1/SCD1 signaling which was found to serve as an important target to attenuate MASLD according to prior research[47–49]. Interestingly, we observed a reduction in the expression of SREBF1 and SCD1 in the CDAHFD group, which aligns with previous publications[50,51]. However, SREBF1/SCD1 signaling is a key pathway in lipogenesis and is typically considered activated in MASH[47]. This discrepancy may be attributed to the inability of CDAHFD-fed mice to secrete TG and cholesterol from the liver, a result of impaired lipoprotein synthesis caused by choline deficiency and reduced methionine[50]. The accumulation of TG and cholesterol within hepatocytes likely induces negative feedback regulation, suppressing the expression of SREBF1 and SCD1. Autophagy is another key biological process associated with cellular degradation and recycling that is positively regulated by AMPK signaling[40,52]. Recent studies have shown that autophagy is impaired in the livers of MASLD patients[53,54]. More importantly, restoring autophagy can alleviate liver steatosis and decrease lipid droplets in mouse models. AKF-PD is found to attenuate paraquat-induced pulmonary fibrosis by regulating autophagy[55] and our study confirmed that AKF-PD also activates autophagy in MASH. Thus, AKF-PD is likely to reduce lipogenesis and promote lipolysis by alleviating hepatic lipid accumulation.

Inflammation is another key driver of MASH progression. The underlying mechanism is extremely complex, involving the release of pro-inflammatory factors, the infiltration of immune cells, and the death of hepatocytes[56]. Of these, NLRP3 inflammasome activation and macrophage infiltration are the two dominant pathogenic processes linked to the development of MASH[57–59]. The NLRP3 inflammasome is an intracellular multiprotein complex in the liver that induces the release of mature IL-1β and pyroptosis[60]. Inhibiting the NLRP3 inflammasome is shown to effectively resolve MASLD[61–63]. The function of macrophages in both innate and adaptive responses stresses their critical role in MASLD[58,64]. Liver macrophages include both tissue-resident Kupffer cells (KCs) and monocyte-derived macrophages recruited from the systemic circulation[65,66]. Current studies have shown that the initiation of MASH is reliant on KCs, which can recruit blood monocytes to the liver by releasing chemokines and cytokines[56,67]. Interestingly, NLRP3 is highly expressed in macrophages in the MASH liver. Our current research showed that AKF-PD inhibits the NLRP3 inflammasome activation and prevents macrophage infiltration. Thus, AKF-PD exerts anti-inflammatory effects by inhibiting NLRP3 inflammasome activation and macrophage infiltration, further contributing to the resolution of MASH.

Liver fibrosis is the major prognostic determinant of liver-related mortality in MASH[68]. Chronic liver injury leads to the activation of hepatic stellate cells (HSCs), which produce collagen and extracellular matrix to promote fibrogenesis[69]. Hepatic macrophages play a vital function in the pathogenesis of liver fibrosis[70] by releasing several mediators, including TGFβ1, and activating HSCs. TGFβ1 signaling recruits HSCs-specific SMAD proteins and strengthens the transcription of fibrogenic genes[71]. Our study confirmed that AKF-PD

reduced hepatic macrophage infiltration. We also showed for the first time that AKF-PD inhibited TGFβ1/SMAD signaling in the CDAHFD-induced MASH model and extended its potential application.

A recent interim analysis meeting report from the Independent Data Monitoring Committee indicated that the Phase II clinical trial (CTR20211557) of AKF-PD for treating HBV-induced liver fibrosis in China has met its primary endpoints. As a result, participant enrollment for the Phase II trial can be terminated, and preparations for a subsequent Phase III trial may be considered. The therapeutic dose of AKF-PD has demonstrated a favorable safety profile in humans with normal liver function. Furthermore, a Phase I clinical trial of the safety of AKF-PD in a population with abnormal liver function is in progress (CTR20213016). In light of this, we believe that it is necessary to conduct more detailed preclinical studies on AKF-PD in MASH to facilitate its prompt advancement into clinical trials.

However, the current study has some limitations. We did not explore other potential AKF-PD-related mechanisms or verify the effects of this compound in other mouse models of MASLD. In the future, we will further explore the effects and mechanisms of AKF-PD in MASH, including constructing other mouse models to support the clinical application of AKF-PD for MASH patients.

In summary, we did reveal for the very first time that AKF-PD significantly ameliorates MASH in a CDAHFD-fed mouse model by reducing hepatic lipid accumulation, inflammation, and fibrosis. The beneficial effects of AKF-PD are mediated, at least in part, through the activation of AMPK signaling, the inhibition of the NLRP3 inflammasome, and TGFβ1/SMAD pathways. As a result, AKF-PD is validated as a promising candidate for the treatment of MASH.

Methods

Chemical reagents and antibodies

CDAHFD was purchased from Research Diets, Inc. (New Brunswick, USA). AKF-PD was synthesized by Sunshine Lake Pharma Co., Ltd. (Dongguan, China). Detailed information on the antibodies used in this study is found in Table S1.

Animals and treatment

All animal studies were approved by the Institutional Animal Care and Use Committee of Xiangya Hospital, Central South University (No. CSU-2022-0463). All the experimental operations were performed in accordance with relevant regulations and ARRIVE guidelines. Six-week-old male C57BL/6 mice were purchased from Hunan SJA Laboratory Animal Co., Ltd. All mice were maintained under SPF conditions and housed with a 12 h light/dark cycle, at 22 ± 2 °C and 50 ± 10% humidity. After a 1-week acclimatization period, the mice were randomly divided into three groups as follows: (1) chow diet group, (2) CDAHFD group (simultaneously treated with an equal volume of vehicle), and (3) CDAHFD+AKF-PD-treated group (500 mg/kg/d, intragastric administration). The dose and administration method of AKF-PD were established based on prior studies and our group's previous findings[27,30]. AKF-PD was dissolved in the vehicle solvent, 0.5% carboxymethyl cellulose sodium. AKF-PD administration was initiated after 1 week of CDAHFD treatment. Six weeks after modeling, the mice were euthanized with sodium pentobarbital intraperitoneal injection, and the serum was collected and immediately stored at −80 °C until analysis. A portion of the liver was fixed in 10% neutral-buffered formalin for histopathology, and the remaining liver tissue was rapidly frozen in liquid nitrogen for further use.

Biochemistry

Liver tissue was homogenized using ethanol. Tissue homogenate was subsequently centrifuged to obtain the supernatant containing hepatic triglycerides (TG) and total cholesterol (TC). Serum alanine aminotransferase (ALT), aspartate aminotransferase (AST), total bile acid (TBA), hepatic TG, and TC were measured using an automated biochemical analyzer LABOSPECT003 (Hitachi LTD, Tokyo, Japan) at the Department of Clinical Laboratory, Xiangya Hospital.

Histological and immunofluorescence assays

Formalin-fixed liver tissues were dehydrated and embedded in paraffin. Five μm-thick sections were stained with hematoxylin and eosin (H&E) (Solarbio, Beijing, China), Oil red (Solarbio, Beijing, China), and Sirius red (MaoKang Biotechnology, Shanghai, China) according to the manufacturer's instructions.

Immunofluorescence (IF) staining was conducted as previously described[27]. In brief, antigen retrieval was achieved by heating Tris-EDTA buffer in a microwave for 15 min. After incubation with the primary antibody at 4 °C overnight, tissue sections were incubated with the appropriate secondary antibody at 37 °C for 1 h. The samples were then incubated with DAPI (Boster Biological Technology, Wuhan, China) for 5 min for nuclear staining. A laser scanning confocal microscope (ZEISS LSM880; Oberkochen, Germany) was used to capture images.

Oil red, Sirius red, and IF staining were quantified by randomly choosing three fields from captured images per liver specimen (n = 3 per group) and the data were analyzed using Image-Pro Plus 6.0 software (NIH, Bethesda, USA).

RNA extraction and RT-qPCR

Total RNA was extracted from liver tissue using Trizol reagent and cDNA was synthesized from 1000 ng total RNA in a 20-μl reaction solution using the Revert Aid First Strand cDNA Synthesis Kit (Takara Bio Inc., Otsu, Japan). RT-qPCR was performed as previously described[27]. The sequences of primers used for RT-qPCR are listed in Table S2. Genes were normalized to 18S and the results were determined using the $2^{-\Delta\Delta Ct}$ method.

Western blot analysis
Total liver protein was acquired by lysing mouse liver tissues in radioimmunoprecipitation assay buffer (Sigma-Aldrich, Saint Louis, USA) with protease and phosphatase inhibitors (Roche, Basel, Switzerland). Protein concentration was measured using a BCA protein assay kit (Thermo Scientific, Bremen, Germany). Protein (20–40 μg) was separated by 8 or 10% SDS-PAGE according to the molecular weight and transferred to PVDF membranes (0.22 μm). Membranes were blocked with TBST buffer in 5% skim milk for 1 h at room temperature. The membranes were incubated overnight at 4 °C with specific primary antibodies. After washing with TBST, membranes were incubated with specific HRP-conjugated secondary antibodies for 1 h at room temperature. The membranes were visualized using an enhanced chemiluminescence (ECL) system, photographed, and digitized. The same membranes were stripped and reblotted with a specific antibody (p-AMPK and AMPK, p-SMAD2 and SMAD2, p-SMAD3, and SMAD3). Protein levels were normalized to β-tubulin and quantified using Image J 1.51 (Bethesda, MD, USA) (n = six per group). Western blot imaging was performed using the Bio-Rad ChemiDOC^{TM} XRS+ system, with images captured using the Image Lab 6.0.1 software in the Chemi Hi Sensitivity mode and automatic exposure settings. No further adjustments were made to the contrast of the images.

Enzyme-linked immunosorbent assay (ELISA)
IL-1β levels in liver lysates were measured using commercial ELISA kits (MM-0040M1, Meimian, Jiangsu, China) according to the manufacturer's instructions, with results normalized to total protein content.

Network pharmacology analysis
The DisGeNET, GeneCards, and OMIM databases were used to screen pathological targets of MASLD. Likewise, the SIB and ChEMBL databases were used to screen the well-reported pharmacological targets of AKF-PD. A Venn diagram was created to identify potential targets for AKF-PD against MASLD. The STRING database was used to construct a protein-protein interaction (PPI) network. Enrichment analysis of the Kyoto Encyclopedia of Genes and Genomes (KEGG) and Reactome pathways was performed using KOBAS[72]. The KEGG PATHWAY dataset (http://www.genome.jp/kegg/pathway.html) and the Reactome PATHWAY dataset (https://reactome.org/) were used for pathway annotations.

RNA-sequencing
Total RNA was extracted by using the RNeasy kit (QIAGEN, Germantown, USA) from the livers of mice treated with CDAHFD (n=4) and CDAHFD+AKF-PD (n=4). The following RNA-sequencing was performed as previously described[73].

Statistical analysis
All data were expressed as the mean ± SD. Comparisons between groups were assessed using one-way ANOVA analysis followed by Tukey's multiple comparison. GraphPad Prism 9.0 software (San Diego, CA, USA) was used for statistical analyses and a P value <0.05 was considered statistically significant.

Data availability
The datasets used and/or analyzed during the current study are available from the corresponding author on reasonable request.

Received: 11 November 2024; Accepted: 13 March 2025
Published online: 21 March 2025

References
1. Friedman, S. L., Neuschwander-Tetri, B. A., Rinella, M. & Sanyal, A. J. Mechanisms of NAFLD development and therapeutic strategies. *Nat. Med.* **24**, 908–922. https://doi.org/10.1038/s41591-018-0104-9 (2018).
2. Sheka, A. C. et al. Nonalcoholic steatohepatitis: A review. *JAMA* **323**, 1175–1183. https://doi.org/10.1001/jama.2020.2298 (2020).
3. Chen, B. et al. Gut bacteria alleviate smoking-related NASH by degrading gut nicotine. *Nature* **610**, 562–568. https://doi.org/10.1038/s41586-022-05299-4 (2022).
4. Younossi, Z. et al. Global perspectives on nonalcoholic fatty liver disease and nonalcoholic steatohepatitis. *Hepatology* **69**, 2672–2682. https://doi.org/10.1002/hep.30251 (2019).
5. Singh, S. et al. Fibrosis progression in nonalcoholic fatty liver vs nonalcoholic steatohepatitis: a systematic review and meta-analysis of paired-biopsy studies. *Clin. Gastroenterol. Hepatol.* https://doi.org/10.1016/j.cgh.2014.04.014 (2015).
6. Loomba, R., Lim, J. K., Patton, H. & El-Serag, H. B. AGA clinical practice update on screening and surveillance for hepatocellular carcinoma in patients with nonalcoholic fatty liver disease: Expert review. *Gastroenterology* **158**, 1822–1830. https://doi.org/10.1053/j.gastro.2019.12.053 (2020).
7. Ferguson, D. & Finck, B. N. Emerging therapeutic approaches for the treatment of NAFLD and type 2 diabetes mellitus. *Nat. Rev. Endocrinol.* **17**, 484–495. https://doi.org/10.1038/s41574-021-00507-z (2021).
8. Vilar-Gomez, E. et al. Weight loss through lifestyle modification significantly reduces features of nonalcoholic steatohepatitis. *Gastroenterology* https://doi.org/10.1053/j.gastro.2015.04.005 (2015).
9. Powell, E. E., Wong, V. W. & Rinella, M. Non-alcoholic fatty liver disease. *Lancet* **397**, 2212–2224. https://doi.org/10.1016/S0140-6736(20)32511-3 (2021).
10. Fan, J. G., Kim, S. U. & Wong, V. W. New trends on obesity and NAFLD in Asia. *J. Hepatol.* **67**, 862–873. https://doi.org/10.1016/j.jhep.2017.06.003 (2017).
11. Polyzos, S. A., Kountouras, J. & Mantzoros, C. S. Obesity and nonalcoholic fatty liver disease: From pathophysiology to therapeutics. *Metabolism* **92**, 82–97. https://doi.org/10.1016/j.metabol.2018.11.014 (2019).
12. Sanyal, A. J. Past, present and future perspectives in nonalcoholic fatty liver disease. *Nat. Rev. Gastroenterol. Hepatol.* **16**, 377–386. https://doi.org/10.1038/s41575-019-0144-8 (2019).

13. Lefere, S. & Tacke, F. Macrophages in obesity and non-alcoholic fatty liver disease: Crosstalk with metabolism. *JHEP Rep.* **1**, 30–43. https://doi.org/10.1016/j.jhepr.2019.02.004 (2019).
14. Mantovani, A. et al. Glucagon-like peptide-1 receptor agonists for treatment of nonalcoholic fatty liver disease and nonalcoholic steatohepatitis: An updated meta-analysis of randomized controlled trials. *Metabolites* https://doi.org/10.3390/metabo11020073 (2021).
15. Armstrong, M. J. et al. Liraglutide safety and efficacy in patients with non-alcoholic steatohepatitis (LEAN): a multicentre, double-blind, randomised, placebo-controlled phase 2 study. *Lancet* **387**, 679–690. https://doi.org/10.1016/S0140-6736(15)00803-X (2016).
16. Kokkorakis, M. et al. Resmetirom, the first approved drug for the management of metabolic dysfunction-associated steatohepatitis: Trials, opportunities, and challenges. *Metabolism* **154**, 155835. https://doi.org/10.1016/j.metabol.2024.155835 (2024).
17. Yuan, Q. et al. Fluorofenidone attenuates tubulointerstitial fibrosis by inhibiting TGF-beta (1)-induced fibroblast activation. *Am. J. Nephrol.* **34**, 181–194. https://doi.org/10.1159/000329080 (2011).
18. Wang, L. H. et al. Fluorofenidone attenuates diabetic nephropathy and kidney fibrosis in db/db mice. *Pharmacology* **88**, 88–99. https://doi.org/10.1159/000329419 (2011).
19. Dai, Q. et al. Fluorofenidone alleviates renal fibrosis by inhibiting necroptosis through RIPK3/MLKL pathway. *Front. Pharmacol.* **11**, 534775. https://doi.org/10.3389/fphar.2020.534775 (2020).
20. Tu, S. et al. Fluorofenidone protects liver against inflammation and fibrosis by blocking the activation of NF-kappaB pathway. *FASEB J.* **35**, e21497. https://doi.org/10.1096/fj.202002402R (2021).
21. Peng, Y. et al. Fluorofenidone attenuates hepatic fibrosis by suppressing the proliferation and activation of hepatic stellate cells. *Am. J. Physiol. Gastrointest. Liver Physiol.* **306**, G253-263. https://doi.org/10.1152/ajpgi.00471.2012 (2014).
22. Song, C. et al. Fluorofenidone attenuates pulmonary inflammation and fibrosis via inhibiting the activation of NALP3 inflammasome and IL-1beta/IL-1R1/MyD88/NF-kappaB pathway. *J. Cell. Mol. Med.* **20**, 2064–2077. https://doi.org/10.1111/jcmm.12898 (2016).
23. Wu, Y. H. et al. Fluorofenidone attenuates bleomycin-induced pulmonary fibrosis by inhibiting eukaryotic translation initiation factor 3a (eIF3a) in rats. *Eur. J. Pharmacol.* **773**, 42–50. https://doi.org/10.1016/j.ejphar.2016.01.006 (2016).
24. Song, C. et al. Fluorofenidone attenuates pulmonary inflammation and fibrosis by inhibiting the Il-11/Mek/Erk Signaling pathway. *Shock* **58**, 137–146. https://doi.org/10.1097/SHK.0000000000001960 (2022).
25. Lv, X. et al. Protective effect of fluorofenidone against acute lung injury through suppressing the MAPK/NF-kappaB pathway. *Front. Pharmacol.* **12**, 772031. https://doi.org/10.3389/fphar.2021.772031 (2021).
26. Tang, Y. et al. Fluorofenidone protects mice from lethal endotoxemia through the inhibition of TNF-alpha and IL-1beta release. *Int. Immunopharmacol.* **10**, 580–583. https://doi.org/10.1016/j.intimp.2010.02.005 (2010).
27. Wang, H. et al. Fluorofenidone ameliorates cholestasis and fibrosis by inhibiting hepatic Erk/-Egr-1 signaling and Tgfbeta1/Smad pathway in mice. *Biochim. Biophys. Acta Mol. Basis Dis.* **1868**, 166556. https://doi.org/10.1016/j.bbadis.2022.166556 (2022).
28. Clifford, B. L. et al. FXR activation protects against NAFLD via bile-acid-dependent reductions in lipid absorption. *Cell Metab.* https://doi.org/10.1016/j.cmet.2021.06.012 (2021).
29. Trauner, M. & Fuchs, C. D. Novel therapeutic targets for cholestatic and fatty liver disease. *Gut* **71**, 194–209. https://doi.org/10.1136/gutjnl-2021-324305 (2022).
30. Peng, Y. et al. The antihepatic fibrotic effects of fluorofenidone via MAPK signalling pathways. *Eur. J. Clin. Invest.* **43**, 358–368. https://doi.org/10.1111/eci.12053 (2013).
31. Matsumoto, M. et al. An improved mouse model that rapidly develops fibrosis in non-alcoholic steatohepatitis. *Int. J. Exp. Pathol.* **94**, 93–103. https://doi.org/10.1111/iep.12008 (2013).
32. Dungubat, E. et al. Effects of caffeine and chlorogenic acid on nonalcoholic steatohepatitis in mice induced by choline-deficient, L-amino acid-defined, high-fat diet. *Nutrients* https://doi.org/10.3390/nu12123886 (2020).
33. Chavez-Talavera, O., Tailleux, A., Lefebvre, P. & Staels, B. Bile acid control of metabolism and inflammation in obesity, type 2 diabetes, dyslipidemia, and nonalcoholic fatty liver disease. *Gastroenterology* https://doi.org/10.1053/j.gastro.2017.01.055 (2017).
34. Fuchs, C. D. & Trauner, M. Role of bile acids and their receptors in gastrointestinal and hepatic pathophysiology. *Nat. Rev. Gastroenterol. Hepatol.* **19**, 432–450. https://doi.org/10.1038/s41575-021-00566-7 (2022).
35. Fang, C. et al. The AMPK pathway in fatty liver disease. *Front. Physiol.* **13**, 970292. https://doi.org/10.3389/fphys.2022.970292 (2022).
36. Paul, B., Lewinska, M. & Andersen, J. B. Lipid alterations in chronic liver disease and liver cancer. *JHEP Rep.* **4**, 100479. https://doi.org/10.1016/j.jhepr.2022.100479 (2022).
37. Chen, C. L. & Lin, Y. C. Autophagy dysregulation in metabolic associated fatty liver disease: A new therapeutic target. *Int. J. Mol. Sci.* https://doi.org/10.3390/ijms231710055 (2022).
38. Qian, H. et al. Autophagy in liver diseases: A review. *Mol. Aspects Med.* **82**, 100973. https://doi.org/10.1016/j.mam.2021.100973 (2021).
39. Filali-Mouncef, Y. et al. The menage a trois of autophagy, lipid droplets and liver disease. *Autophagy* **18**, 50–72. https://doi.org/10.1080/15548627.2021.1895658 (2022).
40. Mihaylova, M. M. & Shaw, R. J. The AMPK signalling pathway coordinates cell growth, autophagy and metabolism. *Nat. Cell Biol.* **13**, 1016–1023. https://doi.org/10.1038/ncb2329 (2011).
41. Kim, Y. C. & Guan, K. L. mTOR: a pharmacologic target for autophagy regulation. *J. Clin. Invest.* **125**, 25–32. https://doi.org/10.1172/JCI73939 (2015).
42. Hu, H. H. et al. New insights into TGF-beta/Smad signaling in tissue fibrosis. *Chem. Biol. Interact.* **292**, 76–83. https://doi.org/10.1016/j.cbi.2018.07.008 (2018).
43. Day, E. A., Ford, R. J. & Steinberg, G. R. AMPK as a therapeutic target for treating metabolic diseases. *Trends Endocrinol. Metab.* **28**, 545–560. https://doi.org/10.1016/j.tem.2017.05.004 (2017).
44. Zhao, P. et al. An AMPK-caspase-6 axis controls liver damage in nonalcoholic steatohepatitis. *Science* **367**, 652–660. https://doi.org/10.1126/science.aay0542 (2020).
45. Hu, M. et al. Salidroside activates the AMP-activated protein kinase pathway to suppress nonalcoholic steatohepatitis in mice. *Hepatology* **74**, 3056–3073. https://doi.org/10.1002/hep.32066 (2021).
46. Yan, L. S. et al. Schisandrin B mitigates hepatic steatosis and promotes fatty acid oxidation by inducing autophagy through AMPK/mTOR signaling pathway. *Metabolism* **131**, 155200. https://doi.org/10.1016/j.metabol.2022.155200 (2022).
47. Zhu, X. et al. Berberine attenuates nonalcoholic hepatic steatosis through the AMPK-SREBP-1c-SCD1 pathway. *Free Radic. Biol. Med.* **141**, 192–204. https://doi.org/10.1016/j.freeradbiomed.2019.06.019 (2019).
48. Li, R. et al. Reducing VEGFB accelerates NAFLD and insulin resistance in mice via inhibiting AMPK signaling pathway. *J. Transl. Med.* **20**, 341. https://doi.org/10.1186/s12967-022-03540-2 (2022).
49. Zhang, J. X. et al. Corosolic acid attenuates hepatic lipid accumulation and inflammatory response via AMPK/SREBPs and NF-kappaB/MAPK signaling pathways. *Am. J. Chin. Med.* **48**, 579–595. https://doi.org/10.1142/S0192415X20500299 (2020).
50. Sugasawa, T. et al. One week of CDAHFD induces steatohepatitis and mitochondrial dysfunction with oxidative stress in liver. *Int. J. Mol. Sci.* https://doi.org/10.3390/ijms22115851 (2021).
51. Matsumoto, K. et al. Hepatic gene expression and functional changes associated with nonalcoholic steatohepatitis. *Mol. Med. Rep.* https://doi.org/10.3892/mmr.2022.12841 (2022).
52. Li, Y. & Chen, Y. AMPK and autophagy. *Adv. Exp. Med. Biol.* **1206**, 85–108. https://doi.org/10.1007/978-981-15-0602-4_4 (2019).

53. Fukuo, Y. et al. Abnormality of autophagic function and cathepsin expression in the liver from patients with non-alcoholic fatty liver disease. *Hepatol. Res.* **44**, 1026–1036. https://doi.org/10.1111/hepr.12282 (2014).
54. Gonzalez-Rodriguez, A. et al. Impaired autophagic flux is associated with increased endoplasmic reticulum stress during the development of NAFLD. *Cell Death Dis.* **5**, e1179. https://doi.org/10.1038/cddis.2014.162 (2014).
55. Jiang, F. et al. Effect of fluorofenidone against paraquat-induced pulmonary fibrosis based on metabolomics and network pharmacology. *Med. Sci. Monit.* **27**, e930166. https://doi.org/10.12659/MSM.930166 (2021).
56. Schuster, S., Cabrera, D., Arrese, M. & Feldstein, A. E. Triggering and resolution of inflammation in NASH. *Nat. Rev. Gastroenterol. Hepatol.* **15**, 349–364. https://doi.org/10.1038/s41575-018-0009-6 (2018).
57. de Carvalho Ribeiro, M. & Szabo, G. Role of the inflammasome in liver disease. *Annu. Rev. Pathol.* **17**, 345–365. https://doi.org/10.1146/annurev-pathmechdis-032521-102529 (2022).
58. Barreby, E., Chen, P. & Aouadi, M. Macrophage functional diversity in NAFLD - more than inflammation. *Nat. Rev. Endocrinol.* **18**, 461–472. https://doi.org/10.1038/s41574-022-00675-6 (2022).
59. Xu, L. et al. Hepatic macrophage as a key player in fatty liver disease. *Front. Immunol.* **12**, 708978. https://doi.org/10.3389/fimmu.2021.708978 (2021).
60. Wan, X., Xu, C., Yu, C. & Li, Y. Role of NLRP3 inflammasome in the progression of NAFLD to NASH. *Can. J. Gastroenterol. Hepatol.* **2016**, 6489012. https://doi.org/10.1155/2016/6489012 (2016).
61. Csak, T. et al. Both bone marrow-derived and non-bone marrow-derived cells contribute to AIM2 and NLRP3 inflammasome activation in a MyD88-dependent manner in dietary steatohepatitis. *Liver Int.* **34**, 1402–1413. https://doi.org/10.1111/liv.12537 (2014).
62. Dixon, L. J., Flask, C. A., Papouchado, B. G., Feldstein, A. E. & Nagy, L. E. Caspase-1 as a central regulator of high fat diet-induced non-alcoholic steatohepatitis. *PLoS ONE* **8**, e56100. https://doi.org/10.1371/journal.pone.0056100 (2013).
63. Wree, A. et al. NLRP3 inflammasome activation is required for fibrosis development in NAFLD. *J. Mol. Med. (Berlin)* **92**, 1069–1082. https://doi.org/10.1007/s00109-014-1170-1 (2014).
64. Liddiard, K. & Taylor, P. R. Understanding local macrophage phenotypes in disease: shape-shifting macrophages. *Nat. Med.* **21**, 119–120. https://doi.org/10.1038/nm.3798 (2015).
65. David, B. A. et al. Combination of mass cytometry and imaging analysis reveals origin, location, and functional repopulation of liver myeloid cells in mice. *Gastroenterology* **151**, 1176–1191. https://doi.org/10.1053/j.gastro.2016.08.024 (2016).
66. Scott, C. L. et al. Bone marrow-derived monocytes give rise to self-renewing and fully differentiated Kupffer cells. *Nat. Commun.* **7**, 10321. https://doi.org/10.1038/ncomms10321 (2016).
67. Krenkel, O. & Tacke, F. Macrophages in nonalcoholic fatty liver disease: A role model of pathogenic immunometabolism. *Semin. Liver Dis.* **37**, 189–197. https://doi.org/10.1055/s-0037-1604480 (2017).
68. Hagstrom, H. et al. Fibrosis stage but not NASH predicts mortality and time to development of severe liver disease in biopsy-proven NAFLD. *J. Hepatol.* **67**, 1265–1273. https://doi.org/10.1016/j.jhep.2017.07.027 (2017).
69. Kumar, S., Duan, Q., Wu, R., Harris, E. N. & Su, Q. Pathophysiological communication between hepatocytes and non-parenchymal cells in liver injury from NAFLD to liver fibrosis. *Adv. Drug Deliv. Rev.* **176**, 113869. https://doi.org/10.1016/j.addr.2021.113869 (2021).
70. Tacke, F. & Zimmermann, H. W. Macrophage heterogeneity in liver injury and fibrosis. *J. Hepatol.* **60**, 1090–1096. https://doi.org/10.1016/j.jhep.2013.12.025 (2014).
71. Hernandez-Gea, V. & Friedman, S. L. Pathogenesis of liver fibrosis. *Annu. Rev. Pathol.* **6**, 425–456. https://doi.org/10.1146/annurev-pathol-011110-130246 (2011).
72. Bu, D. et al. KOBAS-i: intelligent prioritization and exploratory visualization of biological functions for gene enrichment analysis. *Nucleic Acids Res.* **49**, W317–W325. https://doi.org/10.1093/nar/gkab447 (2021).
73. Wu, C. et al. Hepatic BRD4 is upregulated in liver fibrosis of various etiologies and positively correlated to fibrotic severity. *Front. Med. (Lausanne)* **8**, 683506. https://doi.org/10.3389/fmed.2021.683506 (2021).

Acknowledgments

This study was funded by National Natural Science Foundation of China (No. 81974080 and No. 82170640), Natural Science Foundation of Hunan Province (No. 2022JJ30954), Natural Science Foundation of Changsha (No. kq2502051), and Key Research and Development Program of Hunan Province (No. 2022SK2059).

Author contributions

S.P., L.F., J.Z. and H.W. proposed the conception and designed the experiments. J.Z., H.W., Q.W., N.Z. and J.L. performed all of the experiments. J.Z. and H.W. wrote the main manuscript and prepared the figures. L.T., Z.P., and G.H. provided resources. L.F., S.P. and H.W. revised the manuscript and funded this research. All authors reviewed and approved the final submitted manuscript.

Declarations

Competing interests

The authors declare no competing interests.

Additional information

Supplementary Information The online version contains supplementary material available at https://doi.org/10.1038/s41598-025-94401-7.

Correspondence and requests for materials should be addressed to H.W., L.F. or S.P.